ISSN: 2710-0588

Study on Aerodynamic Interference of Tilt-rotor Aircraft at Different Rotor Deflection Angles

Jiayi Li*

Moscow Aviation Institute, Russia

* Corresponding author

Abstract

This paper presents a numerical simulation of a tiltrotor aircraft developed in the United States, examining the aerodynamic interference between the rotors, wings, and fuselage in three flight conditions: forward flight, transition mode, and hover. The study investigates the distribution of the velocity field, pressure field, vorticity field, and streamlines around the aircraft at different rotor tilt angles.

Keywords

Tilt-rotor aircraft, Aerodynamic interference.

1. Introduction

Currently, with the development of megacities, traffic jams on the roads have become a big problem. In addition, with the increasing mobility of the population in economically developed countries, the efficient transportation of passengers and goods within cities and near suburbs has also become a growing urgent need. Among the tasks facing promising urban and intercity air transport, there are such as: transportation of passengers and cargo from point to point within the city and suburbs, emergency response (ambulance, police, fire service, etc.), monitoring of forests, parks, territories of extended industrial zones.

Compared to other modes of transportation, air transport is a promising and emerging sector that is still in its early stages of development and holds great potential for the growth of urban air mobility.

A tilt-rotor aircraft represents a unique type of aircraft that combines the vertical takeoff and landing capabilities of helicopters with the high-speed cruise flight characteristics of propeller-driven airplanes. It has the potential to become an important component of urban air mobility in the future. The tiltrotor can take off and land without the need for a specific airport runway, making it suitable for operation in any environment, whether in hard-to-reach mountainous areas or densely populated urban regions.

The choice of this issue is based on the fact that a tiltrotor has three flight modes: helicopter, transition, and airplane, providing operational advantages of both helicopters and airplanes. However, despite the clear benefits, there are also complex challenges, such as:

1.In helicopter mode, due to the complex aerodynamic interference between the rotor, wing, and fuselage, the induced airflow from the rotor impacts the upper surface of the wing vertically, creating significant negative lift.

2.In all flight modes, the additional swirling airflow from the rotors significantly complicates the flow field near the wing and fuselage, leading to serious unsteady changes in the flow, as well as aerodynamic forces and moments acting on the tiltrotor. In the transition and airplane modes, the aerodynamic interference of the rotors with the fuselage, wing, and tail differs significantly from that in helicopter mode.

ISSN: 2710-0588

2. Purpose of the Study

The aim of this work is to shape the design and study the aerodynamic characteristics of a tilt-rotor aircraft in various flight modes. It focuses on examining the characteristics of aerodynamic interference at different tilt angles.

To achieve the goal set in this work, the following tasks must be accomplished:

1. Develop the design of the tiltrotor.

2. Construct computational grids for the modeling and analysis of the tiltrotor's aerodynamic characteristics in various flight modes.

3. Select an effective CFD method suitable for calculating the aerodynamic characteristics of the tiltrotor in different flight modes.

4. Analyze the aerodynamic characteristics of the tiltrotor in various flight modes. Perform calculations in the transition mode at different rotor tilt angles to study the impact of these angles on the aerodynamic interference between the rotors and the tiltrotor’s airframe elements (wing, tail assembly, and fuselage).

Practical significance of the work: All the aforementioned studies will enable a better understanding of the aerodynamic characteristics of tiltrotors in various flight modes, thereby enhancing the safety, stability, and controllability of such aircraft. This holds significant academic and applied engineering importance for the design of advanced convertible tilt-rotor aircraft.

3. Analysis of the Research Status

As demonstrated by McVeigh [1] and Felker [2], test results in helicopter mode on a 0.658 scale model of the V-22 showed that aerodynamic interference between the wing and the rotor is the cause of rotor thrust loss. According to the data presented in [3], experiments on V-22 models (FS-TRAM) showed that tilting the rotors by 65°–70° can reduce the maximum negative load on the wing to 6%–8% of the rotor thrust. In the work of Srinivasan et al. [4], a CFD numerical method based on Euler equations was used for the first time to model flow fields in helicopter flight mode. The calculated pressure coefficient values on the wing surface showed satisfactory agreement with the experimental data. Cheng Baofeng [5], using an improved momentum source method, studied the aerodynamic characteristics of a tiltrotor in unsteady transition mode and also analyzed the flow of the tiltrotor in helicopter and airplane modes. This type of CFD numerical modeling, based solely on the momentum source method, has the advantages of low computational cost and simplicity of the mesh method. Li Peng [6], based on the new mobile nested grid models system, conducted research on an efficient and highly accurate CFD method for tiltrotors. By applying the developed numerical methods, he performed an in-depth analysis of the aerodynamic design of the tiltrotor and its aerodynamic characteristics in transition mode. Additionally, an initial experimental study was conducted on the flow mechanisms around the tiltrotor blade tips. Zhenlong Wu et al. [7], using CFD, investigated the aerodynamic interference of a scaled-down V-22 tilt-rotor aircraft model in helicopter and transition modes. The velocity field was discretized using a mixed mesh technique and then solved using Reynolds-averaged Navier-Stokes (RANS) equations. Quasi-steady and fully established methods were employed to model the rotor in transition flight mode. Cheng Hao [8] developed a calculation method for predicting the unsteady aerodynamic characteristics of a tiltrotor in transition mode. In this method, the rotor is modeled using disk theory, which allows the influence of individual blades to be ignored. Numerical results show that this method is capable of effectively modeling the aerodynamic characteristics of a tiltrotor in transition mode.

ISSN: 2710-0588

4. Numerical Modeling Methods

Computational fluid dynamics (CFD) is primarily based on solving the Navier-Stokes (N-S) equations. From a physical standpoint, any fluid motion adheres to three fundamental laws: the law of conservation of mass, the law of conservation of energy, and Newton's second law. These fundamental laws can be mathematically expressed as equations, which in their most basic form can be integral equations or partial differential equations.

Governing Equations of Fluid Flow

Continuity Equation: $\frac{\partial \rho}{\partial t}+\nabla \cdot (\rho \mathbf{V})=0$

Momentum equation:

$$\frac{\partial(\rho u)}{\partial t}+\nabla\cdot(\rho u V)=-\frac{\partial P}{\partial x}+\frac{\partial \tau_{xx}}{\partial x}+\frac{\partial \tau_{yx}}{\partial y}+\frac{\partial \tau_{zx}}{\partial y}+\rho f_x$$

$$\frac{\partial(\rho v)}{\partial t}+\nabla\cdot(\rho v V)=-\frac{\partial P}{\partial y}+\frac{\partial \tau_{xy}}{\partial x}+\frac{\partial \tau_{yy}}{\partial y}+\frac{\partial \tau_{zy}}{\partial y}+\rho f_y$$

$$\frac{\partial(\rho w)}{\partial t}+\nabla\cdot(\rho w V)=-\frac{\partial P}{\partial z}+\frac{\partial \tau_{xz}}{\partial x}+\frac{\partial \tau_{yz}}{\partial y}+\frac{\partial \tau_{zz}}{\partial z}+\rho f_z$$

In this work, the k-ω model is used. Menter, by making corrections to the standard two-parameter k-ε turbulence model, proposed the Shear Stress Transport (SST) turbulence model. This model effectively transitions between different zones of flow.

$$\frac{\partial(\rho k)}{\partial t}+\nabla\cdot(\rho U k)=\nabla\cdot\left(\left(\mu+\frac{\mu_t}{\sigma_k}\right)\nabla k\right)+P_k-D_k$$

$$\frac{\partial\ (\rho\omega)}{\partial t}+\nabla\cdot(\rho U\omega)=\nabla\cdot\left(\left(\mu+\frac{\mu_t}{\sigma_k}\right)\nabla\omega\right)+\frac{\gamma}{\nu_t}P_k-\beta\rho\omega^2+2(1-F_1)\frac{\rho\sigma\omega^2}{\omega}\nabla k{:}\,\nabla\omega$$

5. Geometric Model of the Tiltrotor Aircraft

5.1. The parameters of the tilt-rotor aircraft are summarized in the table below:

Parameters	Size
Fuselage Length	10.00 м
Fuselage Width	7.62 м
Fuselage Height	2.25 м
Rotor Diameter	2.00 м
Wing Sweep Angle	-7.5°
Wing Dihedral Angle	4°
Wing Angle of Attack	0°
Distance Between Vertical Stabilizers	3.46 м (42.5°)
Wing Profile	Bell A821201
Rotor Blade Profile	XN Series

5.2. Model Building

(1) Fuselage Modeling

ISSN: 2710-0588

Using the sketch tool in CATIA, the main outline of the fuselage was drawn, including cross-sections for the nose, middle, and tail sections. Afterward, the fuselage surfaces were generated using mesh surface functions and other tools. Based on the parameters of the vertical stabilizer, its outline was sketched, and its 3D model was created using the extrusion function.

(2) Wing Modeling

The wing's cross-sectional outline was drawn according to the wing profile. Since the Bell A821201 airfoil was unavailable, a similar profile, the Boeing B-29 root airfoil, was chosen. The profile points were imported into CATIA to create the wing's outline, which was then extruded considering the specified angle of attack, forming a 3D wing.

(3) Engine Nacelle and Rotor Modeling

The engine nacelle is a unique structure for a tiltrotor aircraft, housing the engine that drives the main rotor (MR). The upper part of the nacelle features several complex curved surfaces. To create the engine nacelle, the multi-section surface function in CATIA was utilized. Contours of the nacelle were sketched across various cross-sections, and the 3D model was generated using the extrusion function.

As a result, the model of the tiltrotor aircraft was obtained, as shown in the figure 1.

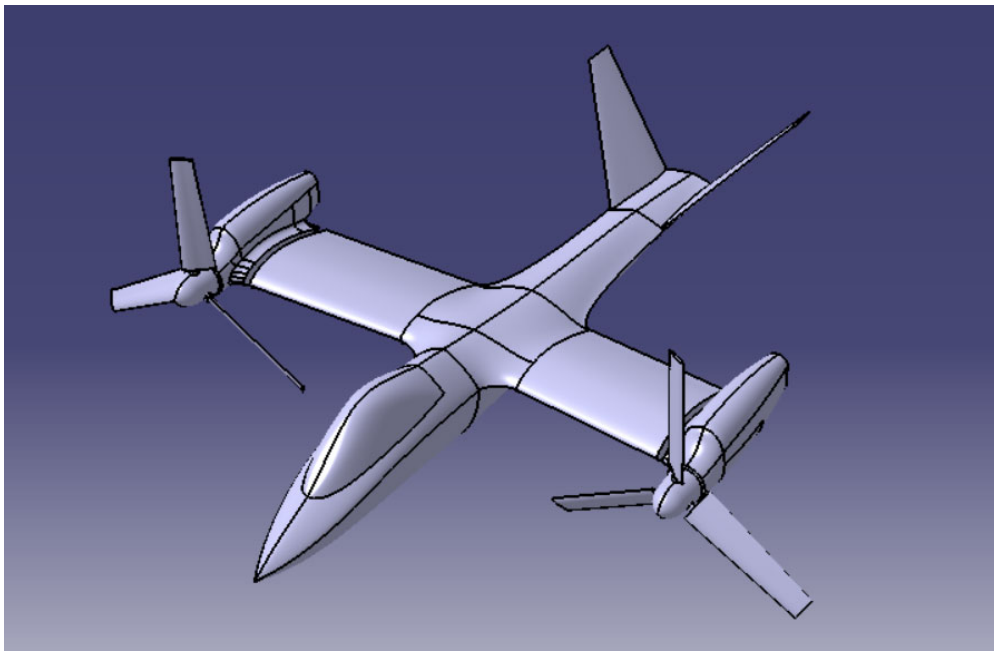

(a)

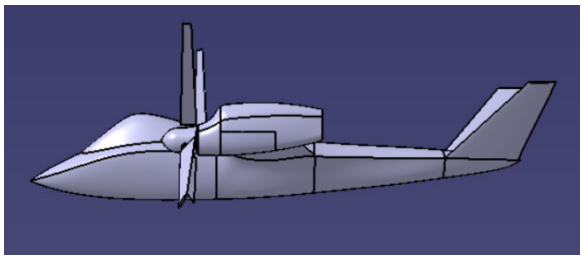

(b)

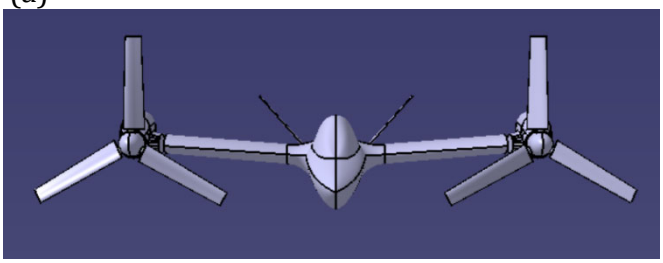

(c)

Figure 1. (a) Axonometric Projection of the Tiltrotor Aircraft
(b) Side projection of the Tiltrotor Aircraft
(c) Front projection of theTiltrotor Aircraft

In this work, SCDM was used for the geometric preparation of complex assemblies. A computational domain was created in the software. First, a cylindrical computational domain

ISSN: 2710-0588

was created, including only the main rotor . Then, another cylindrical computational domain was created, encompassing both the rotor and the power plant. It was necessary to exclude the part containing the wing to simulate the region of rotor interference. Next, a computational domain that included the entire aircraft was created. As a result, five bodies were created, leading to the definition of five computational domains. These domains are shown in Figure 2, where 1 and 2 are the computational domains for the rotors, 3 and 4 for the rotating nacelles, and 5 for the fuselage.

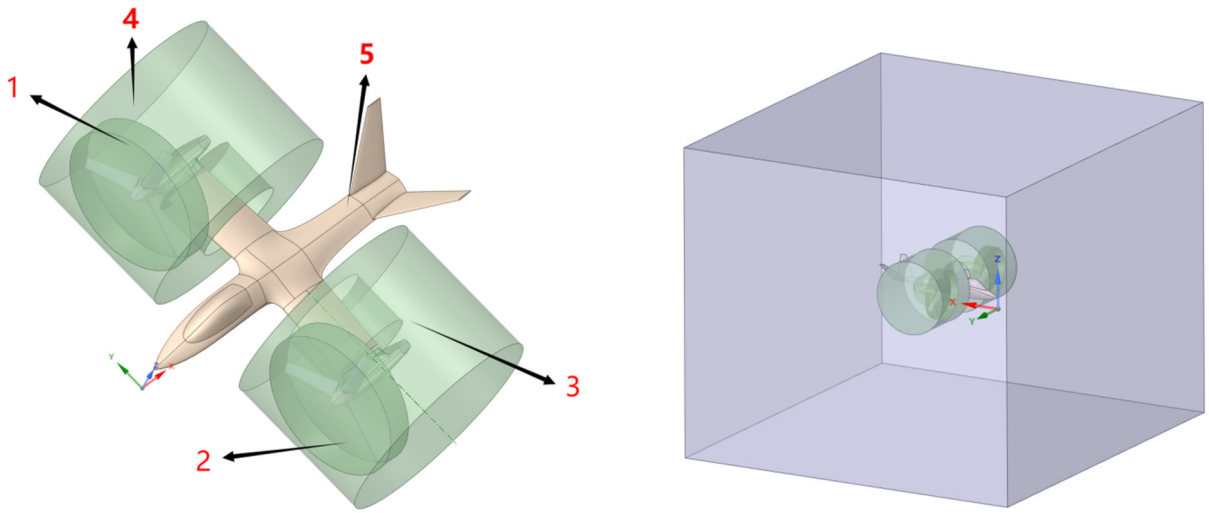

Figure 2. Computational domains of the aircraft

The volumetric mesh is shown in Figure 3

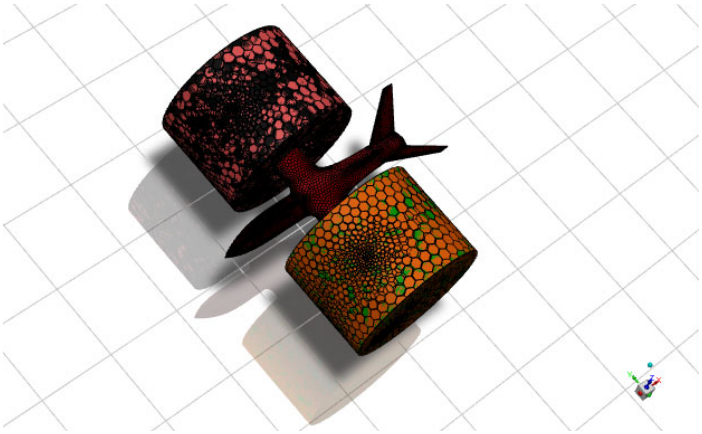

Figure 3. Mesh generation

6. Calculation of the Flow Field in The Aircraft Mode

In the aircraft mode, when a tilt-rotor aircraft is in flight, the engine nacelles are parallel to the fuselage, similar to a conventional propeller-driven airplane. At this moment, since the plane of the rotor disk is perpendicular to the direction of the incoming airflow, the area of the wing and fuselage through which the downwash from the rotor passes is significantly smaller compared to hover mode. Thus, the interference between the rotor wake flow field, the wing, and the fuselage is minimal.

ISSN: 2710-0588

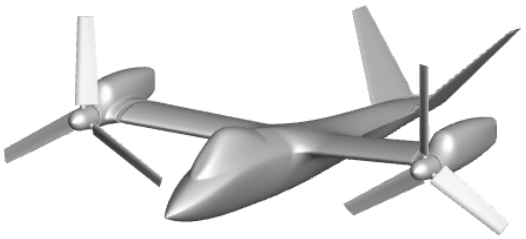

Figure 4. Tilt-rotor aircraft in the aircraft mode..

6.1. Solution Settings

Then the boundary conditions were set: the inlet is set as an inlet with a given speed, and the outlet is set as an outlet with a given pressure. Using the MESH INTERFACE function, interfaces containing the left and right main screws were created, as well as an interface containing the left and right main screws along with a short fuselage. The METHOD solution method uses a method for solving conjugate equations of pressure and velocity. Second-order precision schemes using secondary wind were used for pressure, momentum, turbulent kinetic energy and dissipation factor. In the REPORT DEFINITION, a report is configured on the thrust of the left and right propellers and the lifting force of the aircraft. The residual stresses were adjusted, the grid was initialized and the calculation was started.

6.2. Characteristics of the flow field of a tilt-rotor aircraft in the aircraft mode at an incoming flow velocity V = 125 m/s and a propeller speed of 500 RPM.

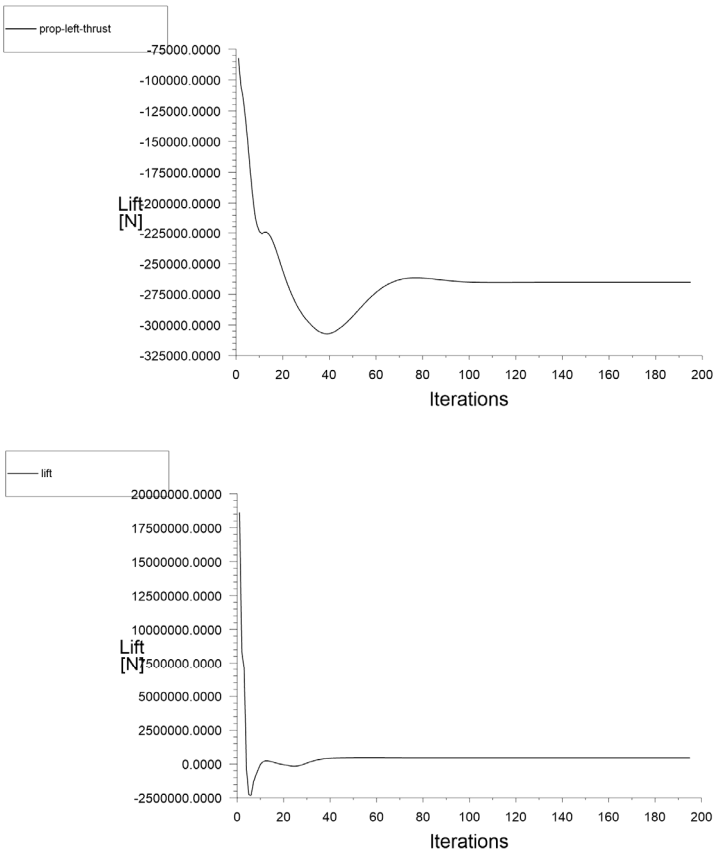

Figure 5. Thrust of the Propeller and Lift of the Aircraft

ISSN: 2710-0588

In Figure 5, it is shown that at a freestream velocity of V = 125 m/s, the propeller thrust is 265,230N, and the lift force of the tilt-rotor aircraft is 453,000 N.

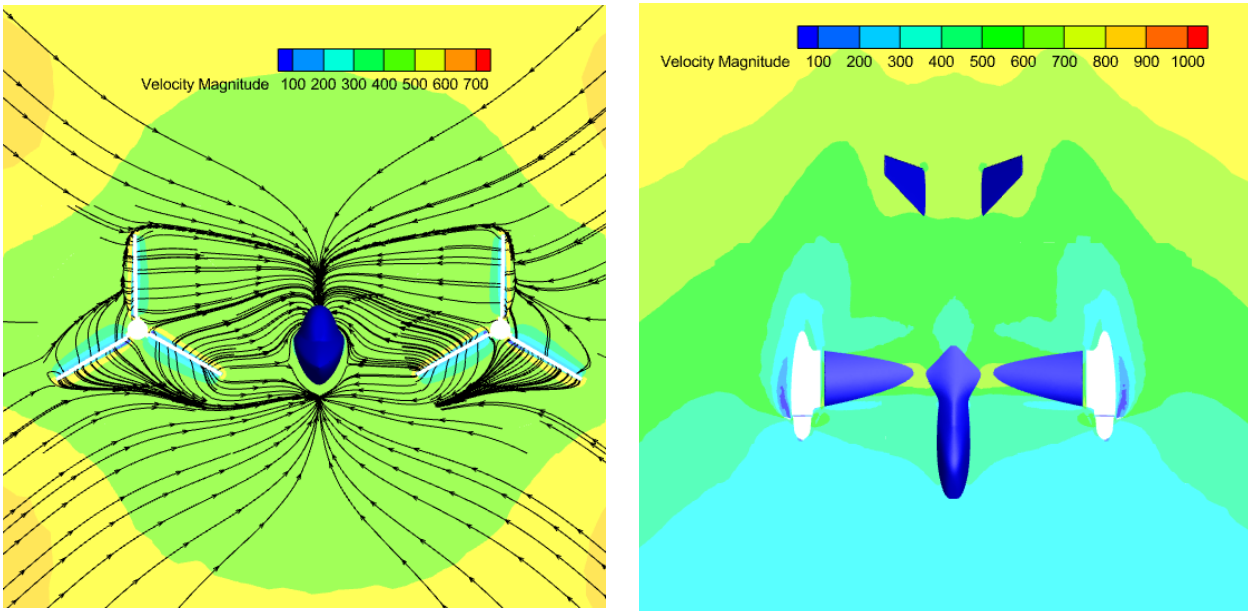

(a) (b)

Figure 6. The velocity distribution of the flow field in the front view (a) and the top view(b).

Figure 6 shows that at an incoming flow velocity of 125 m/s, the velocity is observed around the ends of the propeller blades and is 200 m/s. The speed in the track is also quite high, reaching about 400m/s. The air flows passing on both sides of the fuselage are involved in the movement of the propeller. The figure clearly shows the presence of a low speed zone between the two screw discs.

This phenomenon is explained, on the one hand, by the aerodynamic interference of the wing, which seriously impedes the flow of air; on the other hand, Figure 6 (a) shows that there is also aerodynamic interference between the two propellers, which causes some blocking of the incoming flow on the symmetrical plane of the two propellers, reducing the downward slope of the flow in a tilt-rotor aircraft.

These phenomena indicate significant aerodynamic interference at the leading edge of the wing during the forward flight mode of the tilt-rotor aircraft. In further optimization of the aircraft, a variable cross-section wing can be purposefully used to reduce aerodynamic interference caused by the wing.

From the front view, the streamlines are symmetrical relative to the aircraft, all converging on the symmetrical surface of the aircraft to form a single line. Above the aircraft, the points of convergence are oriented from the nose upward. Below the aircraft, all the streamlines converge at a point close to the lower side of the aircraft.

ISSN: 2710-0588

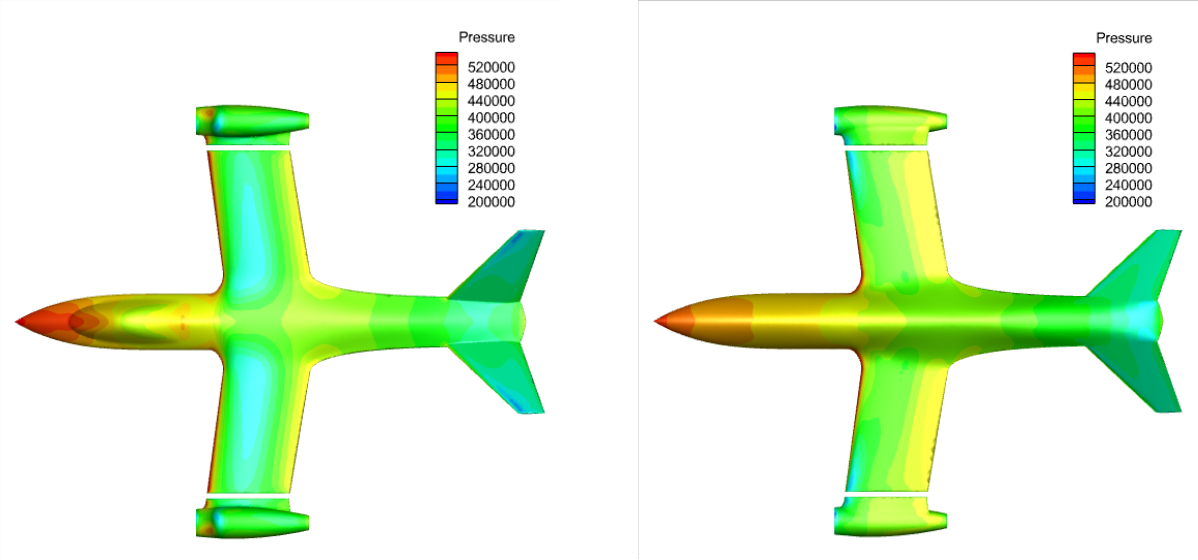

(a)The upper surface (b)The lower surface

Figure 7. Pressure distribution on the upper and lower surface

Figure 7 shows that significant aerodynamic interference occurs on the wing due to the continuous impact of downward flow from the lifting propeller on the wing surface in the horizontal direction. This is especially noticeable at the leading edge of the wing, where a high-pressure zone forms. Besides the geometric shape, the airflow created by the propeller also increases the flow speed over the upper surface of the wing, resulting in reduced pressure.

On the lower surface of the fuselage, there is an area of high pressure, while on the upper surface, there is an area of low pressure.

In the region of the fuselage that is distant from the propeller, pressure changes are relatively small because this area is outside the aerodynamic interference zone of the propeller. The front part of the nacelle also experiences high pressure, which is caused by the impact of the airflow from the propeller on the nacelle.

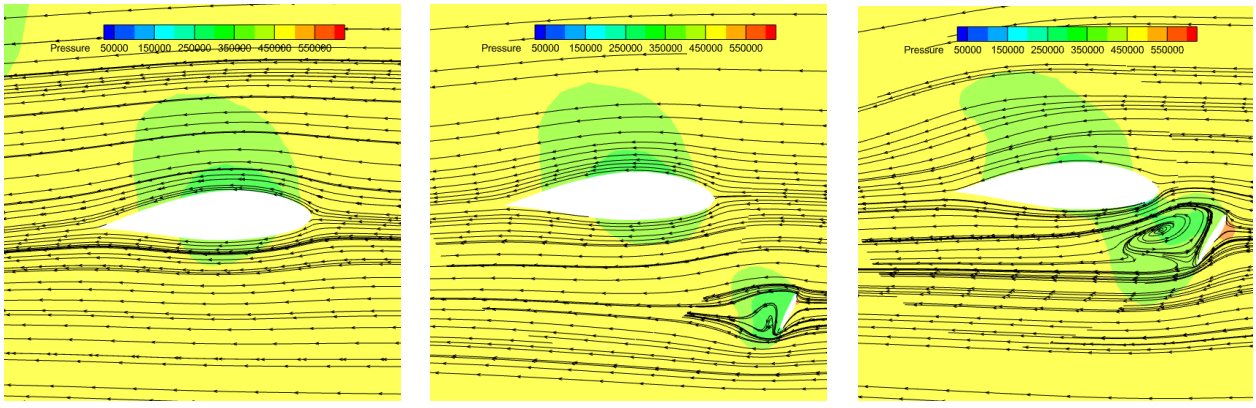

(a) (b) (c)

Figure 8. The pressure distribution along the wing cross-section from the root to the tip (left to right)

Figure 8 shows significant aerodynamic interference between the rotor and the wing. A noticeable downward flow from the rotor is observed around the wing, creating a downward stream. Due to aerodynamic interference between the two propellers, a vortex is present in

ISSN: 2710-0588

front of the wing. Near the wing root, the streamlines are smoother, while closer to the wingtip, the downward flow and vortex become more pronounced and gradually intensify.

There is a significant pressure difference between the upper and lower surfaces of the wing, particularly from the midsection of the wing (B) to the wingtip (C), resulting in most of the wing's lift being generated in this segment.

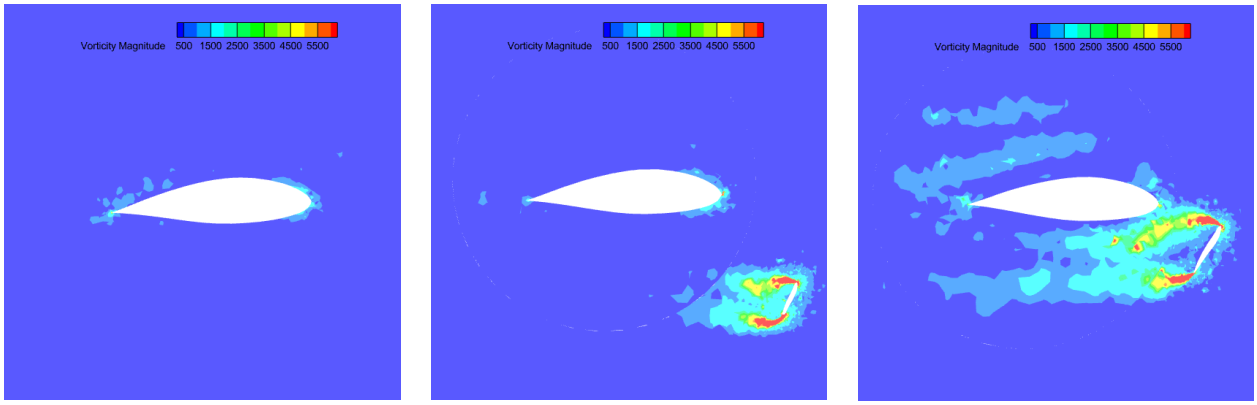

(a) (b) (c)

Figure 9. The vortex distribution across the cross-section from the wing root to the wingtip (left to right)

Figure 9 shows the distribution of vortices on the wing surface, where the tip vortices from the propeller blades (rotor) cause a significant increase in vortex formation on the wing surface. This is due to the high pitch of the rotor blades in the current flight mode of the tilt-rotor aircraft. The shedding vortices from the midsection of the blades interact with the wing surface, leading to the formation of vortices. The detachment of vortices from the blade tips has a noticeable interference effect on the wing.

In Figure 9(b), it is evident that there is a significant accumulation of vortex volume in the midsection and at the root of the wing. Closer to the wingtip, the vortices become more pronounced. This is caused by the interaction of shedding vortices from the midsection of the rotor blades with the wing's leading edge, which, combined with the counterflow, results in complex three-dimensional flow patterns at the wingtip.

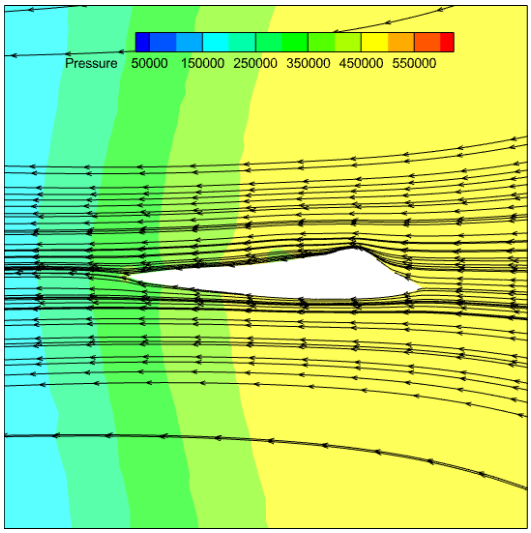

Figure 10. The streamline patterns around the symmetrical plane of the fuselage.

ISSN: 2710-0588

In Figure 10, it is shown that the airflow around the fuselage of the aircraft occurs smoothly, without the formation of vortices.

7. Calculation of the Flow Field in The Transitional Regime.

The propeller rotation speed is 500 RPM, which equals 52.3 rad/s. Time steps of 100 steps are set, with a time interval of 0.01 seconds for the calculations. During the unsteady analysis, the velocity field was analyzed for engine nacelle inclination angles of 30 and 60 degrees.

7.1. Flow Field at V = 61.1 m/s and Engine Nacelle Deflection Angle of 30°

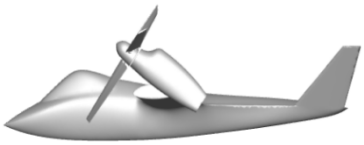

Figure 11. Tilt-rotor aircraft with an Engine Nacelle Deflection of 30°

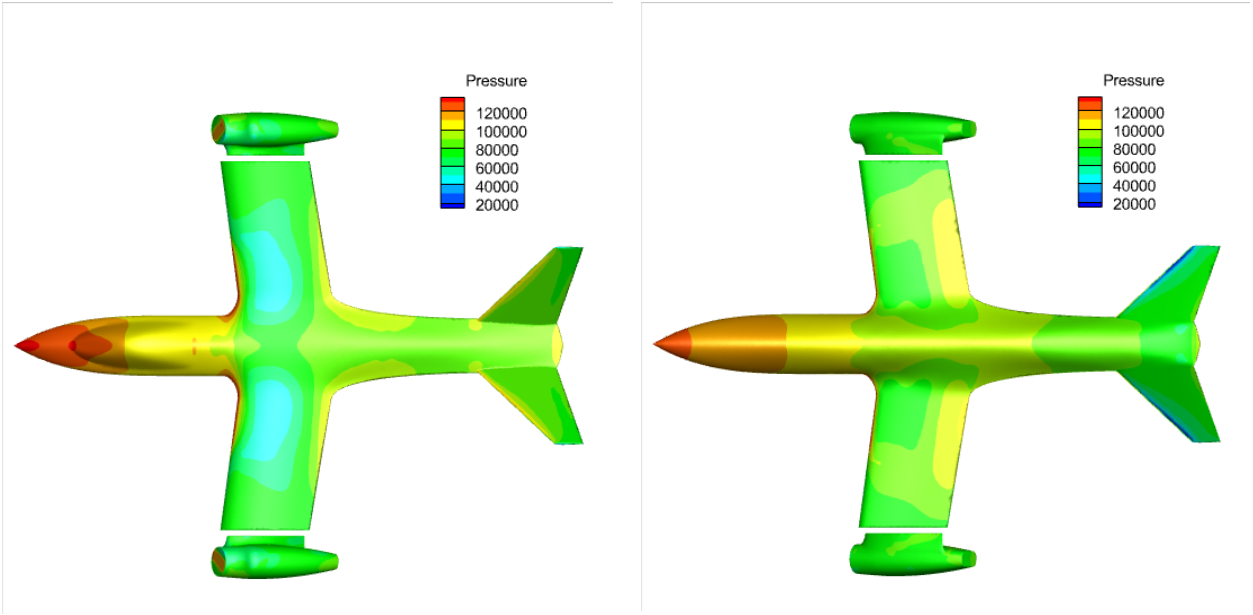

(a)The upper surface (b)The lower surface

Figure 12. Pressure distribution on the upper and lower surface

Figure 12 shows that with a 30-degree deflection angle, at a significant distance from the propeller, a noticeable high-pressure area forms on the leading edge of the wing. This is likely caused by the impact of the flow from the propeller, as described earlier. In addition to geometric factors, the propeller flow also increases the speed over the upper surface of the wing, resulting in reduced pressure. Consequently, a low-pressure area forms on the upper surface of the wing closer to the fuselage, while a high-pressure area forms on the lower surface, particularly noticeable at the trailing edge of the lower surface of the wing. The pressure

ISSN: 2710-0588

distribution on the engine nacelle surface also shows high pressure at the front of the nacelle, which is also due to the impact of the propeller flow.

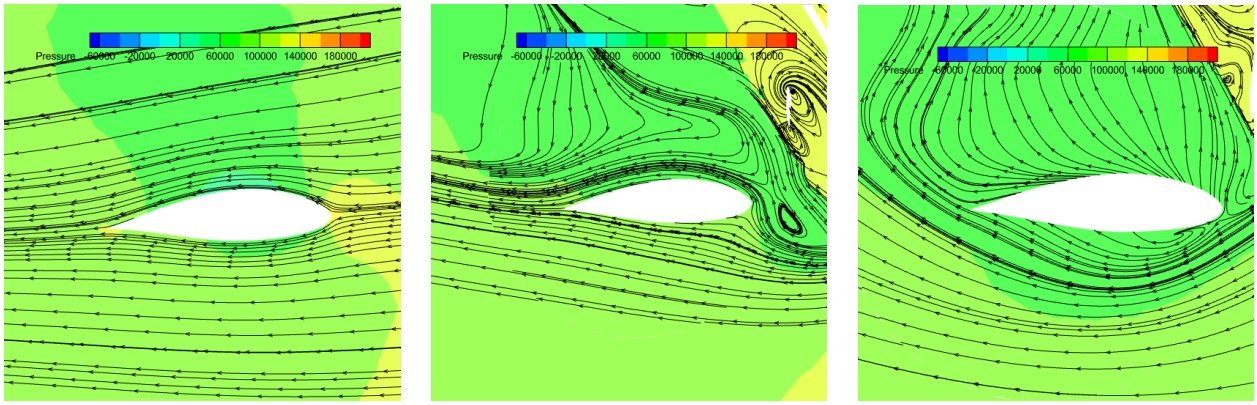

(a) (b) (c)

Figure 13. The pressure distribution along the wing cross-section from the root to the tip (left to right)

Figure 13 shows significant aerodynamic interference between the propellers and the wing. A noticeable downward flow from the rotor is observed around the wing. Due to aerodynamic interference between the two propellers, a vortex is present in front of the wing. Near the wing root, the streamlines are smoother, but as you move towards the wingtip, the flow becomes more pronounced and the vortex gradually increases.

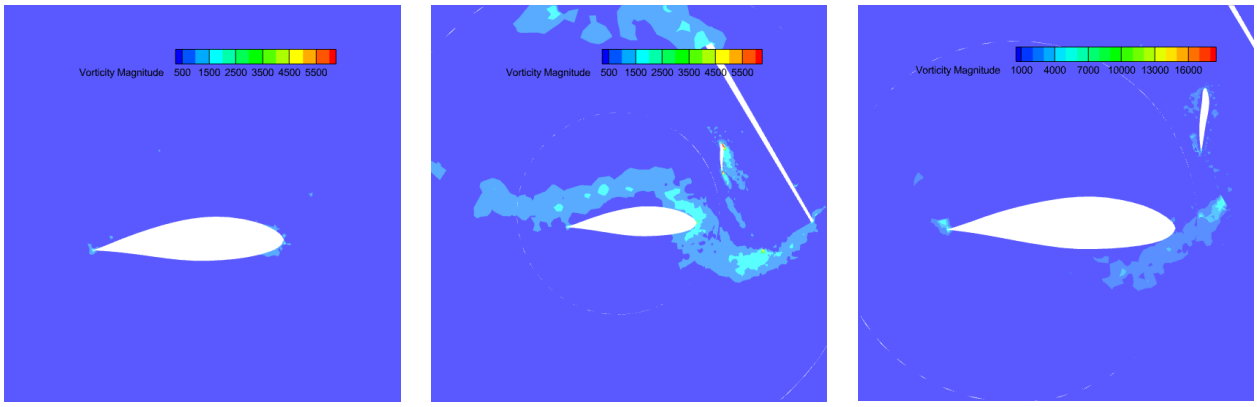

(a) (b) (c)

Figure 14. The vortex distribution across the cross-section from the wing root to the wingtip (left to right).

Figure 14 shows the distribution of vortices on the wing surface, where the impact of vortices from the tips of the rotor blades leads to a significant increase in vortex formations on the wing. This is due to the high overall pitch of the rotor blades in the current mode of the tilt-rotor aircraft, with the shedding vortices from the midsection of the blades interacting with the wing surface, causing vortex formation. The detachment of vortices from the blade tips has a noticeable interference effect on the wing.

In Figure 14(b), it is evident that there is a significant accumulation of vortex volume in the midsection of the wing. This is caused by the interaction of shedding vortices from the midsection of the blades with the leading edge of the wing, which, combined with the counterflow, results in complex three-dimensional flow patterns at the wingtip.

ISSN: 2710-0588

7.2. Flow Field at V = 41.7 m/s and Engine Nacelle Deflection Angle of 60°.

Figure 15. Tilt-rotor aircraft with an Engine Nacelle Deflection of 60°

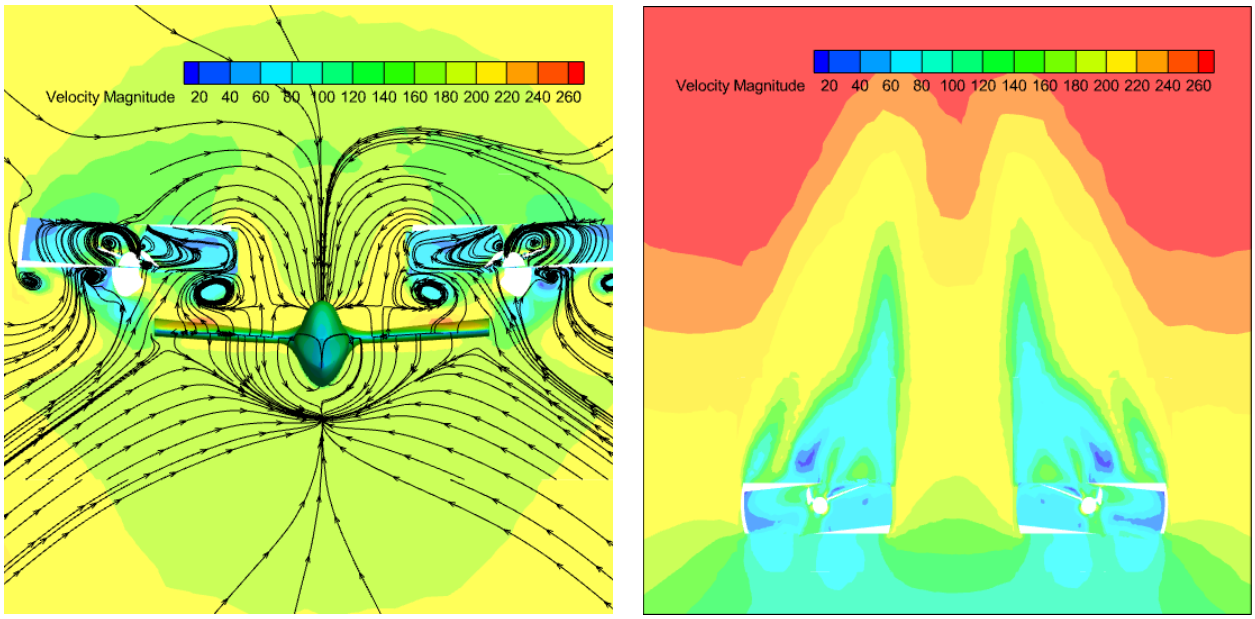

(a) (b)

Figure 16. The velocity distribution of the flow field in the front view (a) and the top view(b)

From the flow left on both sides of the fuselage, air is drawn into the area of the rotating propeller. The figure shows that there is no distinct low-speed zone between the two propeller discs, which is present on the propeller blades.

Figure 16 illustrates that the flow over the aircraft creates a separation: one part of the flow moves downward, while the other moves upward. The distant freestream flow and the flow dispersing above the aircraft form two zones, creating an interface, and both are drawn into the propeller, generating vortices around it. All streamlines converge on the symmetrical plane of the aircraft, with the points of convergence above the aircraft rising from the nose upward. Below the aircraft, all streamlines converge at a single point directly beneath the aircraft.

When a wing is positioned beneath the propeller, it alters the distribution and magnitude of the propeller's induced velocity. The component of the induced velocity directed downward and perpendicular to the wing surface becomes zero as it approaches the wing surface due to blockage, similar to the ground effect of a helicopter.

ISSN: 2710-0588

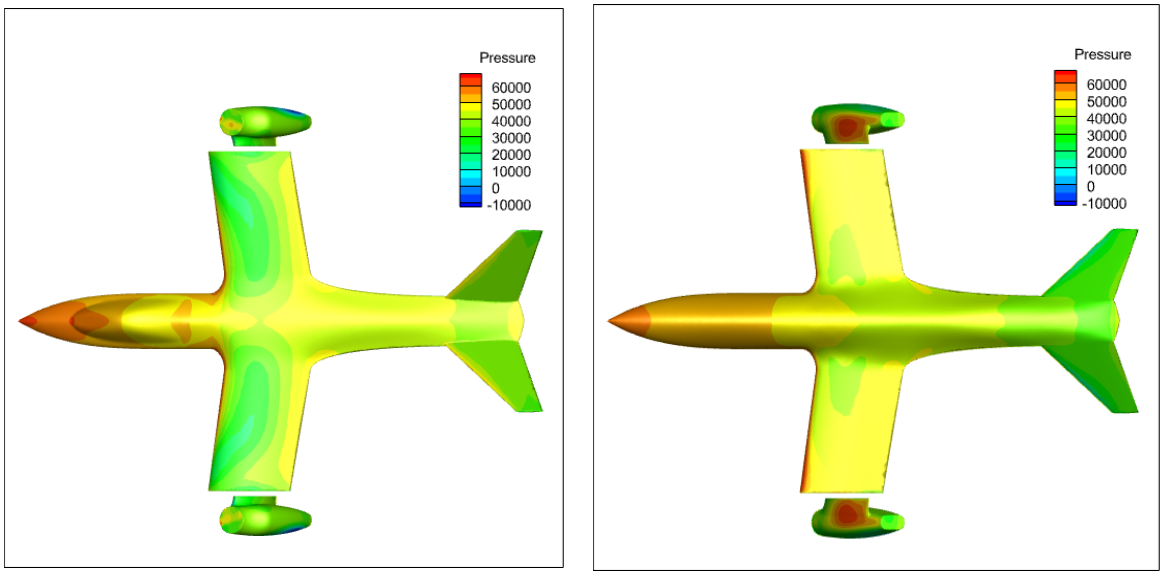

(a)The upper surface (b)The lower surface

Figure 17. Pressure distribution on the upper and lower surface

Figure 17 shows that as the deflection angle increases, the pressure on the wing gradually rises, with the distribution becoming more uniform. At this point, the pressure distribution over the entire upper surface of the wing, from the root to the tip, is quite even.

In addition to geometric shape, the flow created by the propeller also accelerates the airflow over the upper surface of the wing and reduces pressure. In the fuselage area distant from the propeller, the pressure increases, and the pressure distribution becomes more stable due to the minimized impact of the propeller flow. The pressure distribution on the engine nacelle surface indicates that the vortex flow from the root of the rotor significantly deflects towards the nacelle, resulting in a pronounced high-pressure area near the nacelle, closer to the wing. High-pressure zones form at the leading edge of the wing and the front surface of the engine nacelle.

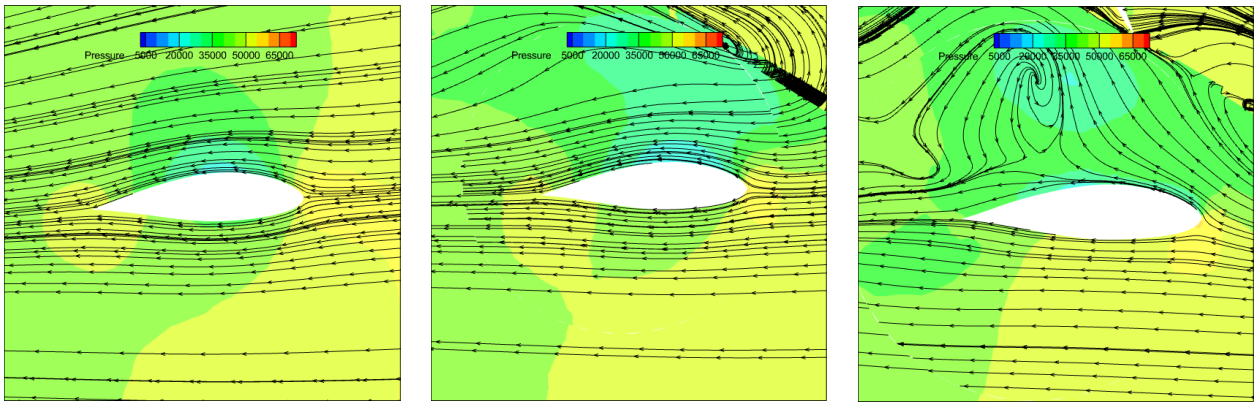

(a) (b) (c)

Figure 18. The pressure distribution along the wing cross-section from the root to the tip (left to right)

Figure 18 shows that there is significant aerodynamic interference between the rotor and the wing. A noticeable downward flow from the rotor affects the wing. Due to aerodynamic interference between the two propellers, a vortex is present in front of the wing. Near the wing root, the streamlines are smoother, but as you move toward the wingtip, the flow becomes more pronounced and the vortex gradually increases.

ISSN: 2710-0588

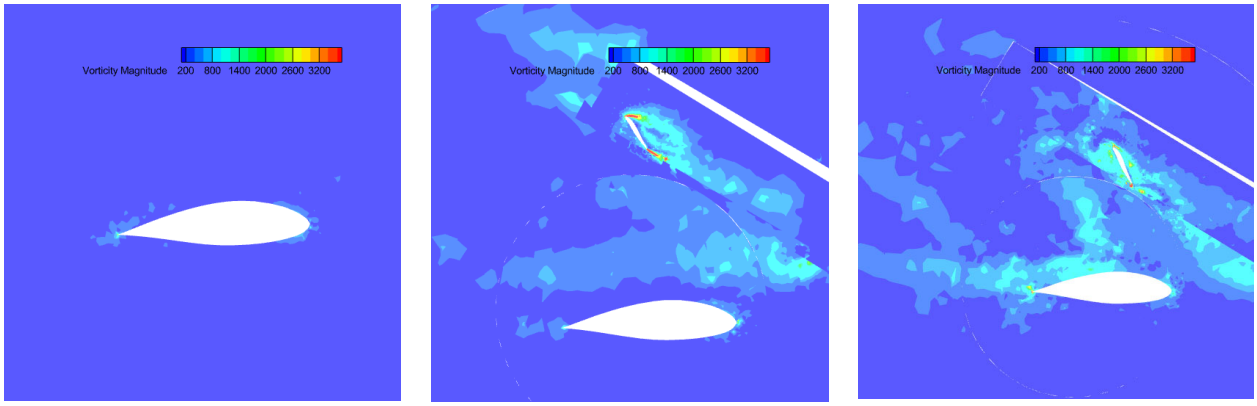

(a) (b) (c)

Figure 19. The vortex distribution across the cross-section from the wing root to the wingtip (left to right).

Figure 19 shows that the vortices at the blade tips significantly increase the vortex motion on the wing surface. This is due to the large overall pitch of the tilt-rotor aircraft in this state, where vortices shed from the midsection of the blades collide with the wing surface, causing noticeable aerodynamic disturbances.

In Figure 19, it is evident that there is a significant accumulation of vortex volume in the midsection of the wing. This is caused by the interaction of shedding vortices from the midsection of the blades with the leading edge of the wing, which, combined with the counterflow, results in complex three-dimensional flow patterns at the wingtip.

8. Calculation of the Flow Field in Hover Mode

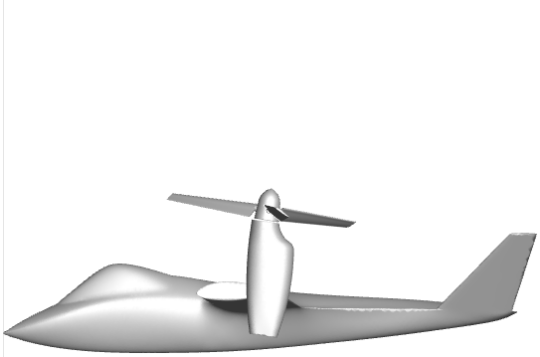

Figure 20. Tilt-rotor aircraft with an Engine Nacelle Deflection of 90°

ISSN: 2710-0588

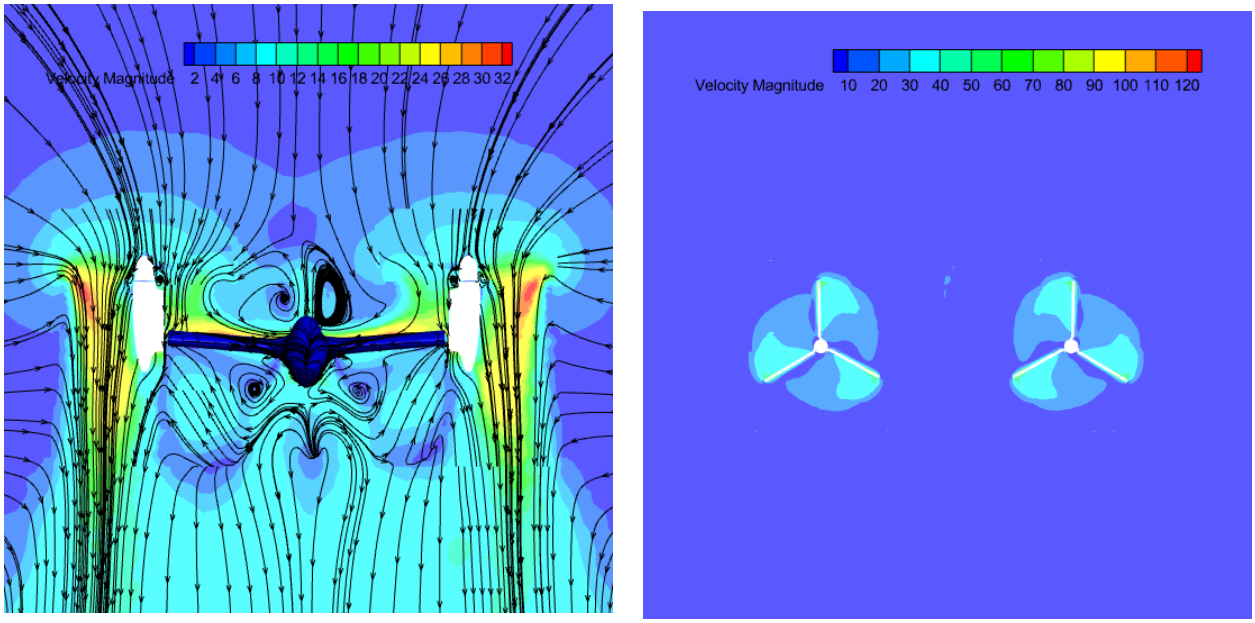

(a) (b)

Figure 21. The velocity distribution of the flow field in the front view (a) and the top view(b)

From the ends of the fuselage, airflows are drawn into the rotating propeller. The graph clearly shows that there is a noticeable low-speed zone between the two propellers. This phenomenon is explained, on one hand, by the wing's impact on the airflow, which significantly impedes the movement of air; on the other hand, as shown in Figure 21), there is also aerodynamic interaction between the two propellers, with the symmetric surfaces between the two propellers creating some blockage of the incoming flow, reducing the downward flow of the tilt-rotor aircraft.

The airflow from the lifting propeller encounters the symmetrical surface of the aircraft, rises, and is then sucked into the propeller.

At a deflection angle of 90° from the propeller blade spiral, the separating vortices significantly disrupt not only the flow between the blades but also cause the lower flow to impact the fixed wing, leading to a three-dimensional blocking effect on the wing surface.

In hover mode, the entire weight of the tilt-rotor aircraft is offset by the lift generated by the rotor. Since the forward flight speed is zero, the downward flow from the lifting rotors strikes vertically against the wing and fuselage, creating additional load. At this point, the interference between the rotor and the fuselage is significantly amplified.

It is observed that in hover mode, the flow field from the rotors takes on a funnel shape. The airflow above the rotors accelerates downward due to suction. The external airflow, encountering no obstacles such as the wing, forms vortex rings at the rotor blade tips. Meanwhile, the internal airflow, passing through the rotor, encounters the wing, impeding its free downward movement. As a result, flows directed along the wing span appear along both sides of the wing.

ISSN: 2710-0588

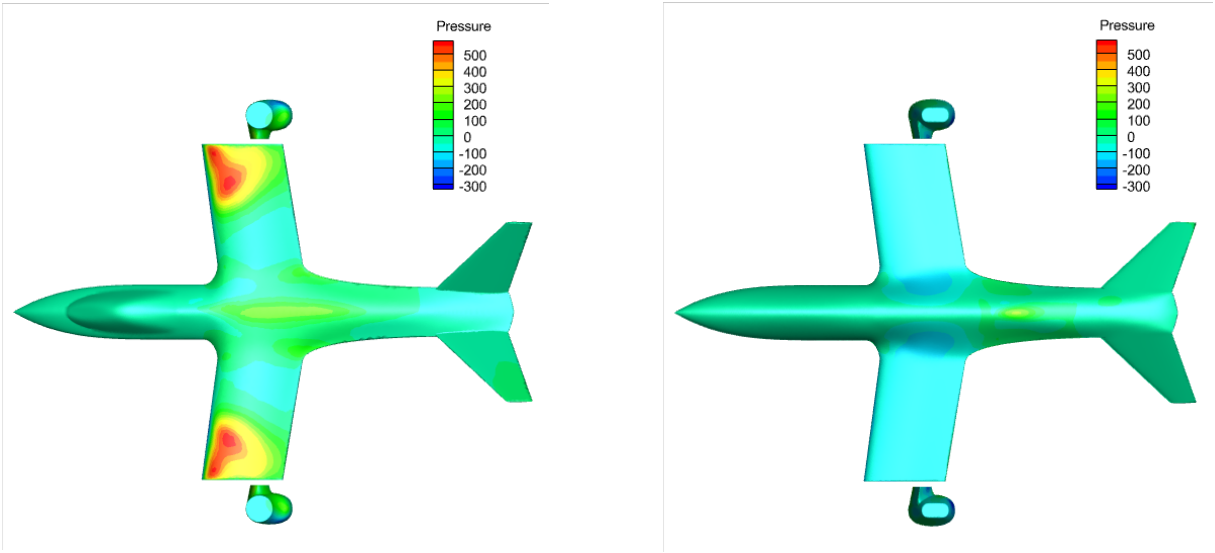

(a)The upper surface (b)The lower surface

Figure 22. Pressure distribution on the upper and lower surface

The interference of the rotor's flow with the upper surface of the wing causes significant changes in pressure on the wing's upper surface, increasing the load on the wing. High pressure was observed near the wingtip.

When a wing is positioned beneath the lifting rotor, it alters the distribution and magnitude of the rotor's induced velocity. The induced velocity directed downward and perpendicular to the wing surface becomes zero as it approaches the wing surface due to blockage, similar to the ground effect of a helicopter.

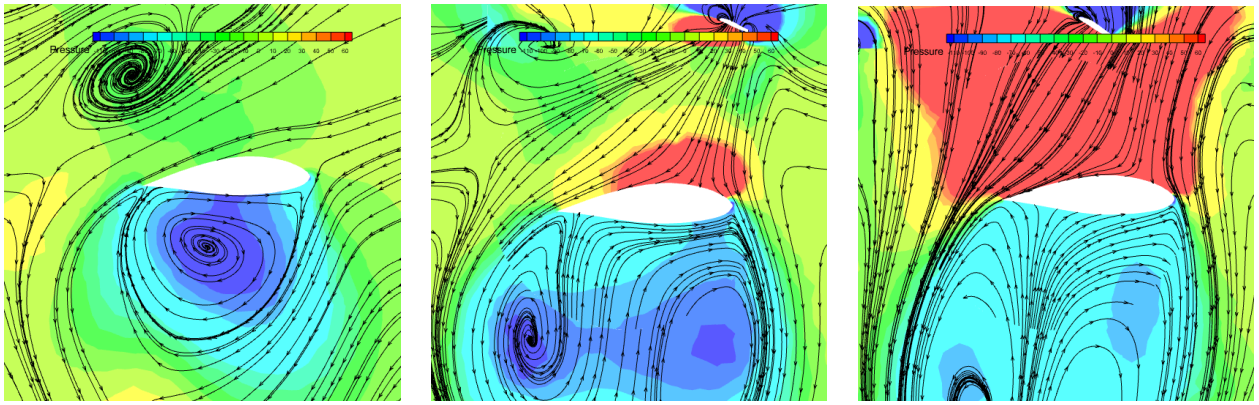

(a) (b) (c)

Figure 23. The pressure distribution along the wing cross-section from the root to the tip (left to right)

It can be seen that at this moment, aerodynamic interference around the wing profile is very significant, and smooth streamlines are not formed. Vortices originating from the rotor are formed around the wing profile.

ISSN: 2710-0588

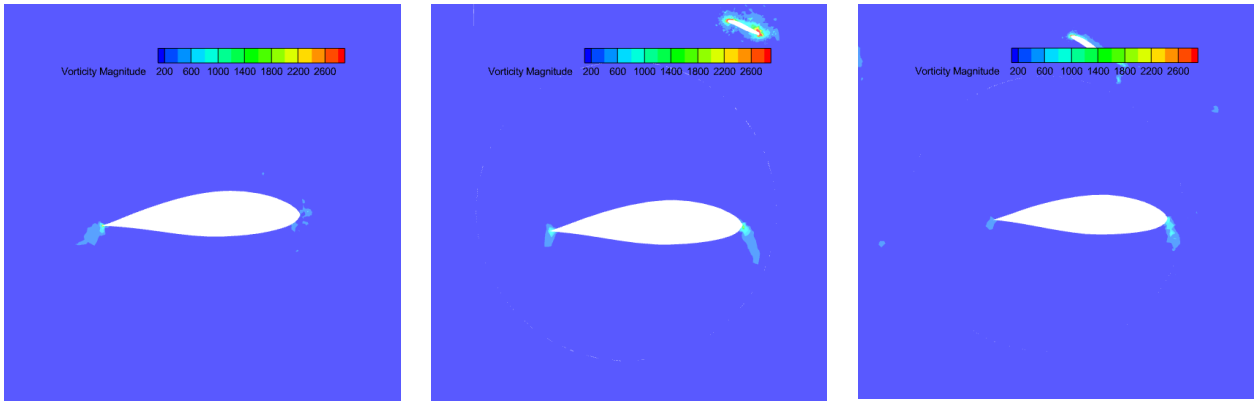

(a) (b) (c)

Figure 24. The vortex distribution across the cross-section from the wing root to the wingtip (left to right).

9. Conclusion

From the velocity lines in the rotor section, it can be seen that there may be a zone of reduced speed between the two rotors. This phenomenon is due to aerodynamic interference between the two rotors, which blocks the flow and reduces the downward flow of the tilt-rotor aircraft, leading to a symmetrical flow setup relative to the aircraft. As the deflection angle increases, the area of the rotor's slipstream decreases. All velocity lines converge into a single line on the aircraft's symmetrical plane.

On the wing, there is pronounced aerodynamic impact caused by the horizontal strike of the rotor's slipstream. Due to the aerodynamic interference of the rotor, an area of increased pressure forms on the upper surface of the wing, causing significant aerodynamic load downward. At a significant distance from the rotor's aerodynamic interference, the change in pressure is relatively small, as the influence of the rotor's flow is minimized. In front of the gondola, there is also an area of increased pressure due to the aerodynamic impact of the rotor's flow. The leading edge of the rotor blade is an area of low pressure with negative pressure, creating thrust, which corresponds to the actual situation.

In various cross-sections of the wing, there is a pronounced mutual influence between the rotor and the wing, evident as significant aerodynamic interference of the rotor on the wing surface. At the wing root, the interference effect is less, while closer to the wingtip, the vortex phenomena become more pronounced, increasing the area of elevated pressure at the front of the wing, and the entire wing section ends up in an area of increased pressure.

The collision of the vortex at the rotor blade tip causes a noticeable increase in the vortex component on the wing surface. This is due to the large overall step of the tilt-rotor aircraft in this position, where the vortex trace detaching from the middle of the blade impacts the wing surface, causing significant aerodynamic interference from the vortex shedding at the blade tip. This is especially evident in the central part of the wing, where significant vortex accumulation occurs in conjunction with the forward flow, leading to complex three-dimensional vortex phenomena at the wingtip. As the deflection angle increases, the number of shedding vortices from the central part of the wing increases, with these vortices impacting the leading edge of the wing, resulting in a larger vortex zone around the wing.

References

[1] McVeigh, M. A., “The V–22 Tiltrotor Large–Scale Rotor Performance/Wing Download Test and Comparison With Theory,” Vertica, Vol. 10, (3/4), 1986, pp. 281–297.

ISSN: 2710-0588

[2] Felker, F., "Wing Download Results from a Test of a 0.658-Scale V–22 Rotor and Wing," Journal of the American Helicopter Society, Vol. 37, (4), October 1992, pp. 58–63.

[3] Young, L., Lillie, D., McCluer, M., Yamauchi, G., and Derby, M., "Insights into Airframe Aerodynamics and Rotor-on-Wing Interactions from a 0.25–Scale Tiltrotor Wind Tunnel Model," American Helicopter Society Aerodynamics, Acoustics, and Test and Evaluation Technical Specialists' Meeting, San Francisco, CA, USA, January 23–25, 2002.

[4] Srinivasan G R, McCroskey W J. Navier-Stokes calculations of hovering rotor flowfields. Journal of Aircraft. 1988, 25(10): 865-874.

[5] Cheng Baofeng. Numerical analysis of the interference flow field of the rotor /wing/fuselage of a tilting tilt-rotor aircraft. Master's Thesis, Nanjing University of Aeronautics and Astronautics learn. 2010.

[6] Li Peng. Analysis of unsteady aerodynamic characteristics and aerodynamic design research of tilt-rotor aircraft [D]. Nanjing University of Aeronautics and Astronautics, 2015.

[7] Chen H. Numerical calculations on the unsteady aerodynamic force of the tilt-rotor aircraft in conversion mode[J]. International Journal of Aerospace Engineering, 2019, 2019: 1-15.

[8] Wu, Z.; Li, C.; Cao, Y. Numerical Simulation of Rotor–Wing Transient Interaction for a Tiltrotor in the Transition Mode. Mathematics 2019, 7, 116.